
Likelihood-Free Gaussian Process for Regression

Yuta Shikuri
Yokohama, Japan
shikuriyuta@gmail.com

Abstract

Gaussian process regression can flexibly represent the posterior distribution of an interest parameter providing that information on the likelihood is sufficient. However, in some cases, we have little knowledge regarding the probability model. For example, when investing in a financial instrument, the probability model of cash flow is generally unknown. In this paper, we propose a novel framework called the likelihood-free Gaussian process (LFGP), which allows representation of the posterior distributions of interest parameters for scalable problems without directly setting their likelihood functions. The LFGP establishes clusters in which the probability distributions of the targets can be considered identical, and it approximates the likelihood of the interest parameter in each cluster to a Gaussian using the asymptotic normality of the maximum likelihood estimator. We expect that the proposed framework will contribute significantly to likelihood-free modeling, especially from the perspective of fewer assumptions for the probability model and low computational costs for scalable problems.

1 Introduction

Gaussian process regression (GPR) is a type of Bayesian nonparametric regression method that allows flexible representation of the posterior distribution of an interest parameter. However, some drawbacks to GPR have been published in the literature, and several reported studies have endeavored to overcome these limitations and contribute to the extended applicability of the method. The most severe drawback of GPR is the computational cost, which is $\mathcal{O}(N^3)$ for data size N . Moreover, the application of GPR to scalable problems has been a significant area of focus in current research. Variational inducing point [Titsias, 2009, Candela and Rasmussen, 2005] to minimize the Kullback–Leibler divergence for approximation of the posterior distribution is the most popular approach among methods for reducing the computational cost and is highlighted in some key works [Csató and Opper, 2000, Shen et al., 2005, Bui and Turner, 2014]. Hensman et al. 2015 extended the likelihood to a non-Gaussian (i.e., free-form likelihood) by estimating the hyperparameters via inducing point framework and Markov-Chain Monte Carlo procedures.

These works have contributed toward establishing a model for the posterior distribution of an interest parameter more flexibly. However, despite the free-form likelihood being a powerful tool, difficulties are encountered when the probability model is unknown. A typical example of this is the modeling of cash flows for investing in financial instruments [Thu and Xuan, 2018, Sidehabi et al., 2016]. The demand for machine learning frameworks for algorithmic trading has been rapidly increasing in recent years. Traders are typically being challenged with predicting asset fluctuations using nonparametric models trained on large amounts of historical data. However, setting the probability model in such a situation is generally infeasible because the cash flows of financial instruments are quite complex.

Demands for likelihood-free modeling exist not only in the field of investments in financial instruments but also in other fields such as ecology and biology. To satisfy this demand, various types of likelihood-free inference methods have been proposed. One idea that is common among these methods is representing the probability distribution of targets through a repetitive process of simulating data

and evaluating the discrepancies between the simulated and observed data [Gutmann and Corander, 2016]. In general, these methods have high computational cost, and we do not know how the parameters affect the discrepancy. Wood 2010 proposed a method that uses the synthetic likelihood to approximate the probability distribution of targets to a multivariate normal distribution by the central limit theorem. The computational cost in their method is more efficient than that of other methods. In addition, the discrepancies between the simulated and the observed data can be evaluated by comparing the individual maximum likelihood estimators for the data. Their method is simple and powerful, and our work is profoundly inspired by it. However, the utility of the method is limited to cases where the generative processes of the targets are clear even though the likelihoods are intractable.

In this study, we propose a novel framework called the likelihood-free Gaussian process (LFGP), which represents the posterior distribution of an interest parameter in the form of a typical GPR without setting the likelihood function directly. We approximate the likelihood to a Gaussian by the framework of GPR and the asymptotic normalities of the maximum likelihood estimators. The concept of our approach is similar to that of [Wood, 2010] from the perspective of the Gaussian approximation. However, we do not assume any generative processes and focus on establishing identically distributed clusters to obtain the maximum likelihood estimators of an interest parameter. For the performance verification of the LFGP, we modeled some pseudo datasets and binary option (BO), which is a type of derivative instrument. Both methods and their results suggest that the LFGP is capable of representing the posterior distribution of an interest parameter even if only little knowledge on its probability model is available. In addition, we show that the LFGP is suitable for scalable problems.

Contribution. We consider that the LFGP will significantly contribute to likelihood-free modeling, especially from the perspective of fewer assumptions for the probability models and lower computational costs for scalable problems.

2 Gaussian Process Regression

Gaussian processes (GPs) are distributions over functions [Rasmussen and Williams, 2006], such that

$$f \sim \mathcal{GP}(\nu(\cdot), k(\cdot, \cdot)), \quad (1)$$

where $\nu : \mathbb{R}^d \rightarrow \mathbb{R}$ is the mean function and $k : \mathbb{R}^d \times \mathbb{R}^d \rightarrow \mathbb{R}$ is the covariance function. Given an observed dataset $\mathbf{D} = \{\mathbf{X}, \mathbf{y}\} = \{\mathbf{x}_i, y_i\}_{i=1}^n$ with $\mathbf{x}_i \in \mathbb{R}^d, y_i \in \mathbb{R}$, the posterior distribution of $\mathbf{f} = \{f(\mathbf{x}_i)\}_{i=1}^n, f : \mathbb{R}^d \rightarrow \mathbb{R}$ is stated as

$$\mathbb{P}(\mathbf{f} | \mathbf{D}, \Lambda, \theta) \sim \mathbb{P}(\mathbf{y} | \mathbf{f}, \Lambda) \mathbb{N}(\mathbf{f} | \nu_{\mathbf{X}}, \mathbf{K}_{\mathbf{X}, \mathbf{X}; \theta}), \quad (2)$$

where $\nu_{\mathbf{X}} = \{\nu(\mathbf{x}_i)\}_{i=1}^n, [\mathbf{K}_{\mathbf{X}, \mathbf{X}'; \theta}]_{s,t} = k(\mathbf{x}_s, \mathbf{x}'_t | \theta), \theta$ are the hyperparameters of the prior distributions, $\Lambda = \{\Lambda(\mathbf{x}_i)\}_{i=1}^n$ are the parameters of the probability model except $\mathbf{f}, \Lambda : \mathbb{R}^d \rightarrow \mathbb{R}^{p-1}$, and $p \in \mathbb{N}$ is the number of parameters.

Training and Prediction. In the context of a GPR, our main concern is maximizing the log marginal likelihood

$$\mathcal{L}(\Lambda, \theta | \mathbf{D}) = \log \mathbb{P}(\mathbf{y} | \mathbf{X}, \Lambda, \theta) = \log \int \mathbb{P}(\mathbf{y} | \mathbf{f}, \Lambda) \mathbb{N}(\mathbf{f} | \nu_{\mathbf{X}}, \mathbf{K}_{\mathbf{X}, \mathbf{X}; \theta}) d\mathbf{f}. \quad (3)$$

The hyperparameters are optimized as

$$\Lambda^*, \theta^* = \arg \max_{\Lambda, \theta} \mathcal{L}(\Lambda, \theta | \mathbf{D}). \quad (4)$$

If the probability model $\mathbb{P}(\mathbf{y} | \mathbf{f}, \Lambda)$ is Gaussian, then we can analytically obtain the gradient $\frac{\partial \mathcal{L}(\Lambda, \theta | \mathbf{D})}{\partial \Lambda}, \frac{\partial \mathcal{L}(\Lambda, \theta | \mathbf{D})}{\partial \theta}$ for the optimization. The form of the log marginal likelihood is given as

$$\mathcal{L}_{\text{normal}}(\Lambda, \theta | \mathbf{D}) = -\frac{1}{2}(\mathbf{y} - \nu_{\mathbf{X}})^T \mathbf{K}^{-1}(\mathbf{y} - \nu_{\mathbf{X}}) - \frac{1}{2} \log |\mathbf{K}| - \frac{n}{2} \log(2\pi), \quad (5)$$

where $\mathbf{K} = \mathbf{K}_{\mathbf{X}, \mathbf{X}; \theta} + \Lambda, \Lambda = \sigma \mathbf{I}_n, 0 < \sigma \in \mathbb{R}$. In addition, the posterior distribution of $\mathbf{f}^* = \{f(\mathbf{x}_i^*)\}_{i=1}^{n^*}$ for a new input $\mathbf{X}^* = \{\mathbf{x}_i^*\}_{i=1}^{n^*}$ with $\mathbf{x}_i^* \in \mathbb{R}^d$ is Gaussian. Further, its mean and

variance are given as

$$\mathbb{E}[\mathbf{f}^* | \mathbf{D}, \mathbf{X}^*, \boldsymbol{\theta}^*, \sigma^*] = \boldsymbol{\nu}_{\mathbf{X}^*} + \mathbf{K}_{\mathbf{X}^*, \mathbf{X}; \boldsymbol{\theta}^*} (\mathbf{K}_{\mathbf{X}, \mathbf{X}; \boldsymbol{\theta}^*} + \sigma^* \mathbf{I}_n)^{-1} (\mathbf{y} - \boldsymbol{\nu}_{\mathbf{X}}), \quad (6)$$

$$\text{Var}[\mathbf{f}^* | \mathbf{D}, \mathbf{X}^*, \boldsymbol{\theta}^*, \sigma^*] = \mathbf{K}_{\mathbf{X}^*, \mathbf{X}^*; \boldsymbol{\theta}^*} + \sigma^* \mathbf{I}_{n^*} - \mathbf{K}_{\mathbf{X}^*, \mathbf{X}; \boldsymbol{\theta}^*} (\mathbf{K}_{\mathbf{X}, \mathbf{X}; \boldsymbol{\theta}^*} + \sigma^* \mathbf{I}_n)^{-1} \mathbf{K}_{\mathbf{X}, \mathbf{X}^*; \boldsymbol{\theta}^*}, \quad (7)$$

where σ^* is the optimized value of σ . Despite these simplifications, GPRs significantly contribute toward modeling various problems flexibly. However, the computational cost $\mathcal{O}(n^3)$ for the inverse matrix computation \mathbf{K}^{-1} is unacceptable from the view of scalability, and the probability model $\text{P}(\mathbf{y} | \mathbf{f}, \boldsymbol{\Lambda})$ is unknown in some cases.

Covariance Function. The radial basis function (RBF) kernel is a basic covariance function that can be written as

$$k_{\text{RBF}}(\mathbf{x}_s, \mathbf{x}'_t | \boldsymbol{\theta}) \equiv C \exp\left(-\frac{1}{2}(\mathbf{x}_s - \mathbf{x}'_t)^T \text{diag}(\mathbf{l})^{-2}(\mathbf{x}_s - \mathbf{x}'_t)\right), \quad (8)$$

where $\boldsymbol{\theta} = \{C, \mathbf{l}\}$, $\mathbf{l} = \{l_j\}_{j=1}^d$, $0 < C, l_j \in \mathbb{R}$ for all j . The covariance functions can be designed flexibly by combining multiple simpler functions. For example, Lee et al. 2018 proved that a GP with a specific covariance function is equivalent to the function of a deep neural network with infinitely wide layers. However, the covariance functions are limited to positive semi-definite types, which sometimes prevent the ability to design them freely. The Euclidean distance space (\mathbb{R}^d, d_E) between two points $(\mathbf{x}_s, \mathbf{x}'_t)$ in the RBF kernel $\exp(-\frac{1}{2}d_E(\mathbf{x}_s, \mathbf{x}'_t)^2)$ cannot be replaced by an uneven distance space [Feragen et al., 2015], where $d_E : \mathbb{R}^d \times \mathbb{R}^d \rightarrow \mathbb{R}$. To address this, some works [Guhaniyogi and Dunson, 2016, Calandra et al., 2016] transformed the original feature space to a new space instead of designing the covariance function directly.

3 Likelihood-Free Gaussian Process

In this section, we discuss the mechanism of the LFGP. As the premise of this discussion, we assume that the targets are independent, the set of parameters and the set of probability distributions have a one-to-one correspondence, the Fisher information matrix is a regular matrix, and $\nu(\cdot) \equiv 0$.

3.1 Approximation to Gaussian

To approximate the likelihood to a Gaussian using the asymptotic normality of the maximum likelihood estimator, we consider assigning the data points $\mathbf{D} = \{\mathbf{x}_i, y_i\}_{i=1}^n$ to m clusters, i.e., $\boldsymbol{\pi} = \{\pi_i\}_{i=1}^n$, $\pi_i \in \{1, 2, \dots, m\}$. If the targets $\mathbf{y} = \{y_i\}_{i=1}^n$ are identically distributed in each cluster and the size n_h of each cluster is sufficiently large, then the maximum likelihood estimators $\mathbf{y}_\boldsymbol{\pi} = \{y_h^\pi\}_{h=1}^m$ of the interest parameters $\mathbf{u} = \{f(\mathbf{z}_h)\}_{h=1}^m$ in the centroids $\mathbf{Z} = \{\mathbf{z}_h\}_{h=1}^m$, $\mathbf{z}_h \in \mathbb{R}^d$ of the clusters approximately follow the Gaussian distribution:

$$\mathbf{y}_\boldsymbol{\pi} \sim \text{N}(\mathbf{y}_\boldsymbol{\pi} | \mathbf{u}, \boldsymbol{\Sigma}_\boldsymbol{\pi}), \quad (9)$$

where $\boldsymbol{\Sigma}_\boldsymbol{\pi} = \text{diag}(\sigma_1^2, \sigma_2^2, \dots, \sigma_m^2)$, $\sigma_h^2 = \frac{1}{n_h} \mathbb{E}_y[(\frac{\partial}{\partial f(\mathbf{z}_h)} \log \text{P}(y | f(\mathbf{z}_h), \boldsymbol{\Lambda}(\mathbf{z}_h)))^2]^{-1} \sim \mathcal{O}(\frac{1}{n_h})$ for all h [Lehmann, 1999].

Identical Distribution. We evaluate the parameter consistency by the geometric mean $r(\boldsymbol{\pi}, \mathbf{Z} | \mathbf{D}, \boldsymbol{\theta})$ of the correlations between the data points and centroids in each cluster, i.e.,

$$r(\boldsymbol{\pi}, \mathbf{Z} | \mathbf{D}, \boldsymbol{\theta}) \equiv \left(\prod_h \prod_{\pi_i=h} \frac{k(\mathbf{x}_i, \mathbf{z}_h | \boldsymbol{\theta})}{\sqrt{k(\mathbf{x}_i, \mathbf{x}_i | \boldsymbol{\theta})k(\mathbf{z}_h, \mathbf{z}_h | \boldsymbol{\theta})}} \right)^{\frac{1}{n}}. \quad (10)$$

If all the data points of a cluster are equivalent to its centroid, then $-\log r(\boldsymbol{\pi}, \mathbf{Z} | \mathbf{D}, \boldsymbol{\theta}) = 0$. We optimize $m, \boldsymbol{\pi}, \mathbf{Z}$ to maximize $r(\boldsymbol{\pi}, \mathbf{Z} | \mathbf{D}, \boldsymbol{\theta})$ under the constraint that the size of each cluster exceeds n_0 :

$$m^*(\boldsymbol{\theta}), \boldsymbol{\pi}^*(\boldsymbol{\theta}), \mathbf{Z}^*(\boldsymbol{\theta}) = \arg \min_{\substack{m, \boldsymbol{\pi}, \mathbf{Z} \\ n_1, n_2, \dots, n_m \geq n_0}} -\log r(\boldsymbol{\pi}, \mathbf{Z} | \mathbf{D}, \boldsymbol{\theta}). \quad (11)$$

In this discussion, we assume that the approximation of the likelihood to a Gaussian holds for $-\log r(\pi^*(\theta), Z^*(\theta) | D, \theta) \leq \delta$ and $n_h \geq n_0$ for all h . Furthermore, we approximate Σ_π as $\sigma_h^2 \sim \mathcal{O}(\frac{1}{n_h}) \leq \mathcal{O}(\frac{1}{n_0}) \simeq 0$.

Training and Prediction. Based on these assumptions, the log marginal likelihood is given as

$$\mathcal{L}_{\text{free}}(\theta | D, \pi, Z) = -\frac{1}{2} \mathbf{y}_\pi^T \mathbf{K}_{Z, Z; \theta}^{-1} \mathbf{y}_\pi - \frac{1}{2} \log |\mathbf{K}_{Z, Z; \theta}| - \frac{n}{2} \log(2\pi). \quad (12)$$

We optimize θ to maximize the log marginal likelihood $\mathcal{L}_{\text{free}}(\theta | D, \pi, Z)$ under the constraints of the aforementioned assumptions:

$$\theta^* = \underset{-\log r(\pi^*(\theta), Z^*(\theta) | D, \theta) \leq \delta}{\arg \max_{\theta}} \mathcal{L}_{\text{free}}(\theta | D, \pi^*(\theta), Z^*(\theta)). \quad (13)$$

The mean and variance of the posterior distribution of $\mathbf{u}^* = \{f(\mathbf{x}_i^*)\}_{i=1}^{n^*}$ for the new input \mathbf{X}^* are

$$\mathbb{E}[\mathbf{u}^* | D, \mathbf{X}^*, \theta^*] = \mathbf{K}_{\mathbf{X}^*, Z^*; \theta^*} \mathbf{K}_{Z^*, Z^*; \theta^*}^{-1} \mathbf{y}_{\pi^*}, \quad (14)$$

$$\text{Var}[\mathbf{u}^* | D, \mathbf{X}^*, \theta^*] = \mathbf{K}_{\mathbf{X}^*, \mathbf{X}^*; \theta^*} - \mathbf{K}_{\mathbf{X}^*, Z^*; \theta^*} \mathbf{K}_{Z^*, Z^*; \theta^*}^{-1} \mathbf{K}_{Z^*, \mathbf{X}^*; \theta^*}. \quad (15)$$

where $\pi^* = \pi^*(\theta^*)$, $Z^* = Z^*(\theta^*)$. It is usually infeasible to optimize θ directly under the given constraints, as in eq. (13). Therefore, we decompose the optimization process into two iterative processes as in algorithm 1. The process of the log marginal likelihood maximization is usually reasonable because the computational cost of the inverse matrix is at most $\mathcal{O}(n^3/n_0^3)$. However, distance-based clustering is generally difficult for scalability reasons [Asgharbeygi and Maleki, 2008].

Algorithm 1 Hyperparameter optimization

- 1: **Input:** $D = \{\mathbf{X}, \mathbf{y}\}$, $n_0, \delta, \epsilon, \theta$, **Output:** $\theta_{\text{old}}, \pi, Z$
 - 2: **repeat**
 - 3: $\theta_{\text{old}} \leftarrow \theta$
 - 4: $m, \pi, Z \leftarrow \underset{\substack{m, \pi, Z \\ n_1, n_2, \dots, n_m \geq n_0}}{\arg \min} -\log r(\pi, Z | D, \theta) \triangleright$ Clustering under cluster size constraint.
 - 5: $\theta \leftarrow \underset{\theta}{\arg \max} \mathcal{L}_{\text{free}}(\theta | D, \pi, Z) \triangleright$ Maximizing the log marginal likelihood.
 - 6: **until** $-\log r(\pi, Z | D, \theta) \leq \delta, \mathcal{L}_{\text{free}}(\theta | D, \pi, Z) - \mathcal{L}_{\text{free}}(\theta_{\text{old}} | D, \pi, Z) \leq \epsilon$
-

3.2 Clustering

To reduce the difficulties associated with scalable clustering, we set the RBF kernel to the covariance function. The form of eq. (11) is expressed as follows:

$$m_{\text{RBF}}^*(\theta), \pi_{\text{RBF}}^*(\theta), Z_{\text{RBF}}^*(\theta) = \underset{\substack{m, \pi, Z \\ n_1, n_2, \dots, n_m \geq n_0}}{\arg \min} \sum_h \sum_{\pi_i=h} (\mathbf{x}_i - \mathbf{z}_h)^T \text{diag}(\mathbf{l})^{-2} (\mathbf{x}_i - \mathbf{z}_h). \quad (16)$$

This is equivalent to the linear k-means [Hartigan and Wong, 1979] function, which is computationally light because we can obtain the centroids analytically. The cost is given by $\mathcal{O}(nm)$ [Murphy, 2012]. However, the two discussion points are the size constraint of the clusters generated by linear k-means and representation of the uneven distance.

Constraint. We can obtain the solution of the linear k-means function heuristically and efficiently using the expectation–maximization algorithm. However, assigning data points to clusters under the cluster size constraints is usually difficult. Here, we provide algorithm 2 by applying the idea of x-means [Pelleg and Moore, 2000], which recursively splits a cluster into two clusters by linear k-means until the clusters no longer meet the division conditions. This algorithm enables us to retain the cluster size constraint while maintaining efficiency in the linear k-means process. The computational cost of algorithm 2 is at most $\mathcal{O}(n^2/n_0)$. Therefore, the total cost of algorithm 1 is at most $\mathcal{O}(n^2/n_0 + n^3/n_0^3)$.

Manifold. As shown above, the RBF kernel significantly reduces the computational cost of algorithm 2. However, we cannot guarantee that we can appropriately represent the feature space by

Algorithm 2 Reclusive clustering

```

1: Input:  $X$ , Output:  $\pi, Z \leftarrow RC(X)$ 
2: procedure  $RC(X)$ 
3:   if  $2n_0 > |X|$  then
4:     return the assignment number  $\pi$  and the centroids  $z$  of  $X$ 
5:   else
6:     Split  $X$  into two clusters  $X_1, X_2$  by linear k-means.
7:     If  $\min\{|X_1|, |X_2|\} < n_0$ , then split  $X$  into  $X_1, X_2$  evenly and randomly.
8:     Run  $RC(X_1), RC(X_2)$  recursively.

```

the RBF kernel. Here, the RBF kernel is not capable of representing the uneven distance of the feature space as the covariance matrix must be semi-positive definite. This is a critical drawback when the data points are distributed on manifolds (\mathcal{M}, d_M) embedded in Euclidean space (\mathbb{R}^d, d_E) . To overcome this drawback, we convert the original feature space to a new Euclidean space, which approximately preserves the uneven distances as an option of the LFPG. For this conversion, we use manifold learning methods (e.g., locally linear embedding (LLE) [Saul and Roweis, 2001], Isomap [Schoeneman et al., 2018], and UMAP [McInnes et al., 2018]) that represent the manifold distances among data points based on the k-neighbor graph.

4 Experimental Results

In this section, we demonstrate two experimental results that verify the performance of the LFPG. The computing environment used is Microsoft Windows 10 Pro, 3.6 GHz Intel Core i9 processor, and 64 GB memory. The code to replicate each experiment in this study is available ¹.

4.1 Basic Performance

In this subsection, we present verification of the behavior of the LFPG from two perspectives using a pseudo dataset (table 1). First, we determine the representations of the posterior distributions of some interest parameters. Our interest parameters here depend on the individual problems. The LFPG allows us to model various types of parameters flexibly. Second, we convert the original feature space to a new Euclidean space using UMAP. The feature space sometimes has the structure of a manifold embedded in Euclidean space. However, in the framework of the LFPG, kernels are practically difficult to use, except for the RBF kernel, owing to the computational cost of clustering for scalability. We empirically show that a preprocessing conversion before training reduces this drawback. In our experiments, we do not focus on the performance of each manifold learning method.

Setup. We prepared three pseudo datasets (Cube, Tube, and Roll), which are plotted in n data points. Each dataset consists of two clusters that have different shapes of beta distribution. Parameters mapped by f are mean, median, variance, and skew of beta distribution. Under these experimental conditions, we first train the LFPG on each dataset, for both cases of converted by UMAP and not converted by UMAP. Next, we show the mean of the posterior distribution of each parameter on n^* test data points, replacing n in table 1 with n^* .

Table 1: Pseudo Dataset

Type	Cluster	$x_{i,1}$	$x_{i,2}$	$x_{i,3}$	y_i
Cube	$i \leq \frac{n}{2}$	$U(-2, 0)$	$U(-2, 2)$	$U(-2, 2)$	$Be(1, 4)$
	$i > \frac{n}{2}$	$U(0, 2)$	$U(-2, 2)$	$U(-2, 2)$	$Be(2, 1)$
Tube	$i \leq \frac{n}{2}$	$\cos \frac{4i}{n} \pi + N(0, 0.1)$	$\sin \frac{4i}{n} \pi + N(0, 0.1)$	$U(-2, 2)$	$Be(1, 4)$
	$i > \frac{n}{2}$	$2 \cos \frac{4i}{n} \pi + N(0, 0.1)$	$2 \sin \frac{4i}{n} \pi + N(0, 0.1)$	$U(-2, 2)$	$Be(2, 1)$
Roll	$i \leq \frac{n}{2}$	$\frac{2i}{n} \cos \frac{2i}{n} \pi + N(0, 0.1)$	$\frac{2i}{n} \sin \frac{2i}{n} \pi + N(0, 0.1)$	$U(-2, 2)$	$Be(1, 4)$
	$i > \frac{n}{2}$	$\frac{2i}{n} \cos \frac{2i}{n} \pi + N(0, 0.1)$	$\frac{2i}{n} \sin \frac{2i}{n} \pi + N(0, 0.1)$	$U(-2, 2)$	$Be(2, 1)$

¹<https://github.com/MLPaperCode/LFPG>

Performance. From fig. 1 and fig. 2, the result with UMAP conversion in the case of Cube is some distance away from the true value of each parameter, compared to the result with non-conversion. Meanwhile, the performance with UMAP conversion is superior to non-conversion in the case of Tube and Roll. In particular, the result with non-conversion in the case of Tube is poor. We consider that the hyperparameter search along the Cartesian coordinates is difficult when data points are symmetrically distributed. These results suggest that the feature space should be converted appropriately depending on the specific problem.

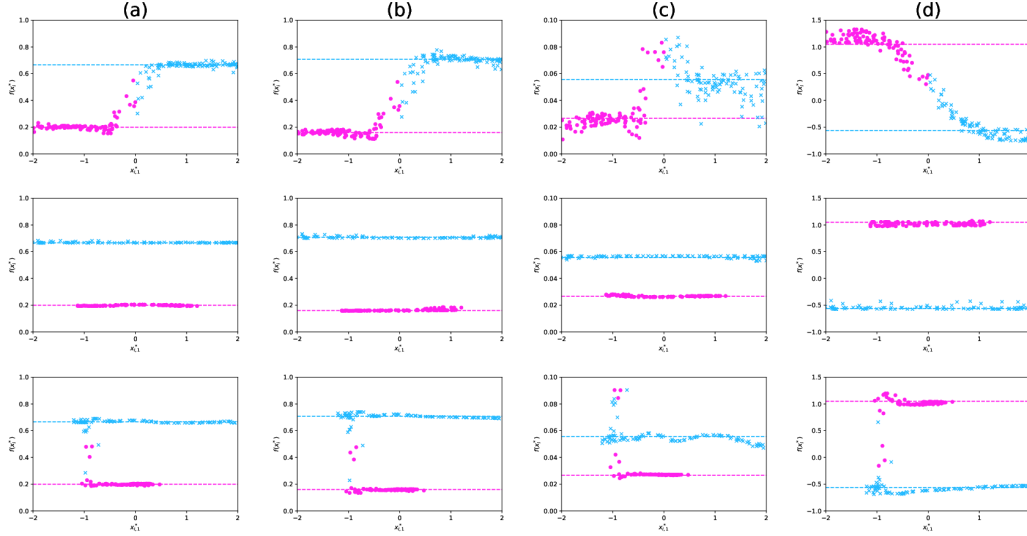


Figure 1: Mean of $f(x_i^*)$ against $x_{i,1}^*$ when dataset is converted by UMAP. Pink: $i \leq \frac{n^*}{2}$, Light blue: $i > \frac{n^*}{2}$. Upper: Cube. Middle: Tube. Lower: Roll. (a) mean. (b) median. (c) variance. (d) skew. $n^* = 200$ data points are plotted. The two dashed lines are the true values of each parameter in each cluster (table 2). $n = 20,000$, $d = 3$, $n_0 = 100$, $\delta = 1$, $\epsilon = 1$, and the k-neighbors of UMAP is 30. Training in the case of Cube did not converge within 20 iterations.

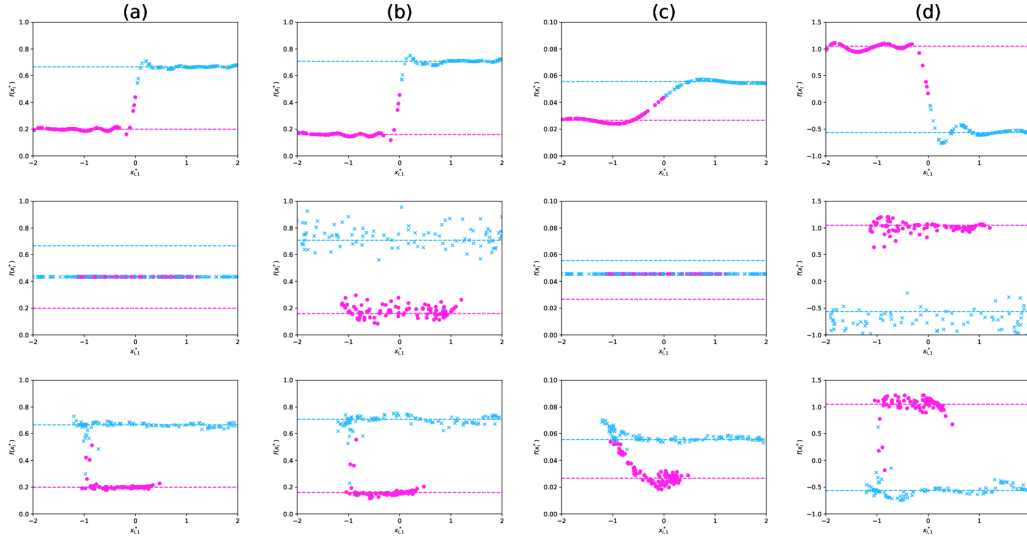


Figure 2: Mean of $f(x_i^*)$ against $x_{i,1}^*$ when dataset is not converted by UMAP. Other conditions are the same as in fig. 1. Training in the case of Roll sometimes did not converge within 20 iterations.

Table 2: True parameters value of beta distribution

Cluster	y_i	Mean	Median	Variance	Skew
$i \leq \frac{n}{2}$	Be(1, 4)	0.200	0.159	0.0267	1.050
$i > \frac{n}{2}$	Be(2, 1)	0.667	0.707	0.0556	-0.566

Scalability. Table 3 suggests that we can train the LFGP on scalable problems using limited iterations and in a realistic timeframe. However, the case wherein $n = 100,000$ and $n_0 = 500$ did not converge because the density of data points in each cluster was sparse. Therefore, n_0 should be set appropriately depending on individual problems.

Table 3: Calculation time and repetition count of algorithm 1. All numerical values in this table are averaged over 10 trials for the cases of Cube, mean, and UMAP non-conversion.

n	$n_0 = 100$		$n_0 = 500$	
	training time [sec]	repetition count	training time [sec]	repetition count
100,000	199 ± 64	5.5 ± 1.8	—*	—*
200,000	684 ± 243	6.2 ± 2.3	665 ± 157	4.8 ± 1.1
400,000	2,752 ± 1,414	7.3 ± 3.8	2,898 ± 1,834	7.1 ± 4.5
800,000	11,490 ± 3,560	8.4 ± 2.7	6,920 ± 2,471	5.2 ± 1.9
1,600,000	44,501 ± 14,805	6.7 ± 2.3	33,704 ± 13,059	6.0 ± 2.3

* Training does not converge within 20 iterations.

4.2 Binary Option

It is generally infeasible to model asset price fluctuations because their probability models are unknown. Herein, we suggest that the LFGP enables representing the percentile points of currency exchange rate fluctuations. To verify the performance of the LFGP, we consider the BO index, which is a simple derivative instrument. The BO index is generally above or below the currency exchange rate fluctuations at any given time. The cash flow of the BO is literally binary in nature, despite being based on the currency exchange rates. Therefore, we can model the cash flow from the BO directly without representing the percentile points of the currency exchange rate fluctuations. Using this feature of the BO, we compare the LFGP with a baseline model. The historical currency exchange rate used here is from OANDA API ².

Rule. In this experiment, we consider the following rules for the BO provided by HighLow ³:

1. Predict whether a currency exchange rate will increase or decrease 30 s in advance.
2. Payout is 1.95 for 1 entry cost when the prediction is correct.
3. A draw is treated as incorrect (significant digits are 0.1 pips).
4. Possible entry timing is Monday to Friday, 8:00–29:00, except for New Year and holidays.

Strategy. The entry asset is GBP/JPY because the frequency of draws is low compared to other currencies. We train the LFGP as a nonparametric model under the hypothesis that there are some patterns of rate movements in short intervals. We do not convert the feature space before the training because of the lack of knowledge of the feature space. The whole procedure is simple:

1. Represent each 48.718 and 51.282 percentile point every 1 min with the LFGP based on every 30 s of rate fluctuation for the previous 30d s.

²<https://developer.oanda.com/rest-live-v20/introduction/>

³<https://trade.highlow.com/>

2. Add stress to the mean of the percentile points based on the posterior distribution

$$\int_{-\infty}^{f_H} \mathcal{N}(f_{48.718}^* | m_{48.718}^*, k_{48.718}^*) df_{48.718}^* = \alpha, \quad (17)$$

$$\int_{-\infty}^{f_L} \mathcal{N}(f_{51.282}^* | m_{51.282}^*, k_{51.282}^*) df_{51.282}^* = 1 - \alpha, \quad (18)$$

where f_H, f_L are the means after stresses of 48.718, 51.282 percentile points of the currency exchange rate fluctuations in 30 s, $f_{48.718}^*, f_{51.282}^*$ are the 48.718, 51.282 percentile points, $m_{48.718}^*, k_{48.718}^*$ are the mean and variance of the posterior distribution of $f_{48.718}^*$, $m_{51.282}^*, k_{51.282}^*$ are the mean and variance of the posterior distribution of $f_{51.282}^*$, and α represents the degree of stress, $0 < \alpha \leq 0.5, \alpha \in \mathbb{R}$.

3. Bet High if the 48.718 percentile point is more than 0.05 pips and bet Low if the 51.282 percentile point is less than -0.05 pips.

Baseline. As a baseline model, we use random forest (RF) [Kam, 1995] which is a nonparametric binary classification model. RF is suitable as a baseline from the perspective of scalability. We represent the individual probabilities of High and Low instead of percentile points and join in the rounds when the probability is higher than $1 - \beta, 0 < \beta \leq 0.5, \beta \in \mathbb{R}$.

Evaluation. The training period is 2017/4/1–2018/3/31, and the evaluation period is 2018/4/1–2019/3/31. From table 4, the LFGP with $d = 10, n_0 = 100$ maximizes the cumulative profit for the evaluation period, and the RF with $d = 20, \text{depth} = 10$.

Table 4: Cumulative profit for the period 2018/4/1–2019/3/31 by the LFGP ($\delta = 1, \epsilon = 1$) and the RF (the number of trees is 100). Profit is 0.95 if the prediction for each entry is correct; loss is 1.00 otherwise. Each value is a maximum in 10 trials in the case of $\alpha = 0.40, \beta = 0.48$.

d	LFGP ($\alpha = 0.40$)			RF ($\beta = 0.48$)		
	$n_0 = 100$	$n_0 = 200$	$n_0 = 300$	depth = 5	depth = 10	depth = 15
10	1,547	999	576	1,021	1,070	336
20	1,047	1,087	1,372	487	1,181	655
30	796	1,408	1,264	263	936	848

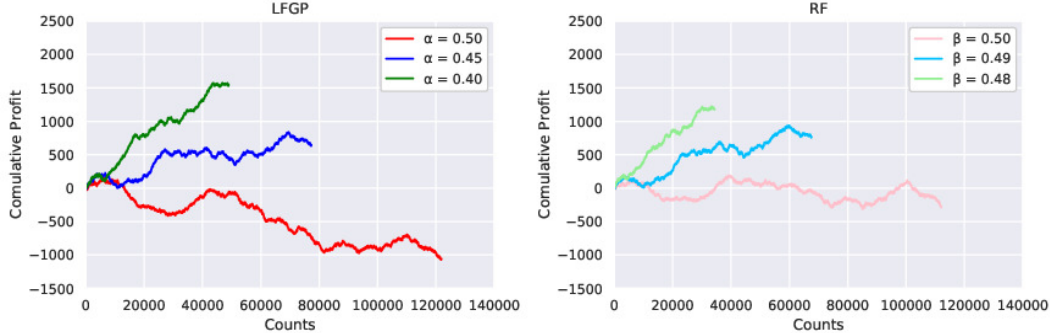


Figure 3: Cumulative profit against entry counts for the period 2018/4/1–2019/3/31. Left: LFGP ($d = 10, n = 314,088, n^* = 313,500, n_0 = 300$). Right: RF ($d = 20, n = 312,828, n^* = 312,250, \text{depth} = 10$). Other conditions are the same as in table 4.

Backtesting. The training period is 2017/4/1–2018/3/31, and the backtesting period is 2019/4/1–2020/3/31. In addition to the evaluation results, fig. 4 suggests that the smaller the value of α and β , the greater the cumulative profit against entry count, and the performances of both LFGP and RF are similar. This suggests that the LFGP is capable of representing the posterior distribution of percentile points without knowledge of the probability distribution of the currency exchange rate fluctuation.

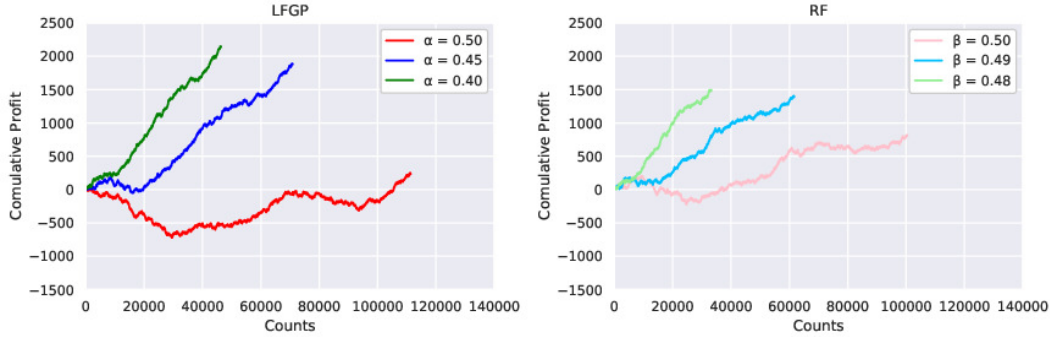


Figure 4: Cumulative profit against entry counts for the period 2019/4/1–2020/3/31. Left: LFGP ($d = 10, n = 314,088, n^* = 316,663, n_0 = 300$). Right: RF ($d = 20, n = 312,828, n^* = 315,398, \text{depth} = 10$). Other conditions are the same as in fig. 3.

5 Conclusion

In this study, we proposed the LFGP, which is a framework for likelihood-free modeling. The main concept of the LFGP is the approximation of the likelihood in each identically distributed cluster to a Gaussian using the asymptotic normality of the maximum likelihood estimator. Compared to existing methods, this approximation exhibits fewer assumptions for the probability models and lower computational costs for scalable problems. However, we emphasize that the asymptotic normality is based on the assumptions that targets are independent, the set of parameters and the set of probability distributions have a one-to-one correspondence, and the Fisher information matrix is a regular matrix. Although considering whether these assumptions are valid for individual problems is necessary, we expect that the proposed method will contribute to likelihood-free modeling in several fields. A typical application is the modeling of cash flows for investing in financial instruments. Cash flows are quite complex, unlike binary options in general. At present, we are continuing our experiments to gain actual profits from the foreign exchange (FX) and not only by means of backtesting. We expect to report the results of the extended work in the near future.

Broader Impact

This study could have a positive impact in terms of stimulating the investment market. Novice investors should learn numerous techniques, which is sometimes a barrier to joining in investment markets. Algorithmic trading might reduce the barrier with a lower fee than professional funds. Further, a concentration risk may occur if investors use similar algorithmic trading models. We should be cautious as algorithmic trading could break the investment market.

Acknowledgement

I wish to thank Dr. Naoki Hamada, Dr. Junpei Komiyama, Dr. Takashi Ohga, Atsushi Suyama, Kevin Noel, Tomoaki Nakanishi, Kohei Fukuda, Masahiro Asami, Daisuke Kadowaki, Yuji Hiramatsu, Hirokazu Iwasawa, and Korki Tomizawa for invaluable advice provided during the writing of this paper. I would also like to thank Editage for their high-quality English language editing. I am grateful to my family for supporting my research activities.

References

- Michalis K. Titsias. Variational learning of inducing variables in sparse gaussian processes. *Proceedings of Machine Learning Research*, 5:567–574, April 2009.
- Joaquin Q. Candela and Carl E. Rasmussen. A unifying view of sparse approximate gaussian process regression. *Journal of Machine Learning Research*, 6:1939–1959, December 2005.

- Lehel Csató and Manfred Opper. Sparse representation for gaussian process models. In *Proceedings of the 13th International Conference on Neural Information Processing Systems*, pages 423–429, Cambridge, MA, USA, December 2000. MIT Press.
- Yirong Shen, Andrew Y. Ng, and Matthias Seeger. Fast gaussian process regression using kd-trees. In *Proceedings of the 18th International Conference on Neural Information Processing Systems*, pages 1225–1232, Cambridge, MA, USA, December 2005. MIT Press.
- Thang D. Bui and Richard E. Turner. Tree-structured gaussian process approximations. In *Proceedings of the 27th International Conference on Neural Information Processing Systems*, pages 2213–2221, Cambridge, MA, USA, December 2014. MIT Press.
- James Hensman, Alexander G. de G. Matthews, Maurizio Filippone, and Zoubin Ghahramani. Mcmc for variationally sparse gaussian processes. In *Proceedings of the 28th International Conference on Neural Information Processing Systems*, pages 1648–1656, Cambridge, MA, USA, December 2015. MIT Press.
- Thuy Nguyen Thi Thu and Vuong D. Xuan. Forex trading using supervised machine learning. *International Journal of Engineering and Technology*, 7(4.15):400–404, 2018.
- Sitti W. Sidehabi, Indrabayu Amirullah, and Sofyan Tandungan. Statistical and machine learning approach in forex prediction based on empirical data. In *Proceedings of International Conference on Computational Intelligence and Cybernetics*. IEEE, November 2016.
- Michael U. Gutmann and Jukka Corander. Bayesian optimization for likelihood-free inference of simulator-based statistical models. *Journal of Machine Learning Research*, 17(125):1–47, January 2016.
- Simon N. Wood. Statistical inference for noisy nonlinear ecological dynamic systems. *NATURE*, 466(7310):1102–1104, August 2010.
- Carl E. Rasmussen and Christopher K. I. Williams. *Gaussian Processes for Machine Learning*. The MIT Press, 2006.
- Jaehoon Lee, Yasaman Bahri, Roman Novak, Samuel S. Schoenholz, Jeffrey Pennington, and Jascha Sohl-Dickstein. Deep neural networks as gaussian processes. In *Proceedings of International Conference on Learning Representations*, Vancouver, BC, Canada, May 2018.
- Aasa Feragen, Francois Lauze, and Søren Hauberg. Geodesic exponential kernels: When curvature and linearity conflict. In *Proceedings of Computer Vision and Pattern Recognition*, pages 3032–3042, Boston, MA, USA, October 2015. IEEE.
- Rajarshi Guhaniyogi and David B. Dunson. Compressed gaussian process for manifold regression. *Journal of Machine Learning Research*, 17(1):2472–2497, January 2016.
- Roberto Calandra, Jan Peters, Carl Edward Rasmussen, and Marc Peter Deisenroth. Manifold gaussian processes for regression. In *Proceedings of International Joint Conference on Neural Networks*, pages 3338–3345, Vancouver, BC, Canada, July 2016. IEEE.
- E. L. Lehmann. *Elements of Large-Sample Theory*. Springer, . edition, 1999.
- Nima Asgharbeygi and Arian Maleki. Geodesic k-means clustering. In *Proceedings of International Conference on Pattern Recognition*, pages 1–4. IEEE, December 2008.
- J. A. Hartigan and M. A. Wong. A k-means clustering algorithm. *Applied statistics*, 28(1):100–108, January 1979.
- Kevin P. Murphy. *Machine Learning: A Probabilistic Perspective*. MIT Press, . edition, 2012.
- Dan Pelleg and Andrew W. Moore. X-means: Extending k-means with efficient estimation of the number of clusters. In *Proceedings of International Conference on Machine Learning*, pages 727–734. Morgan Kaufmann Publishers, June 2000.
- Lawrence K. Saul and Sam T. Roweis. An introduction to locally linear embedding. *Journal of Machine Learning Research*, 7, January 2001.
- Frank Schoeneman, Varun Chandola, Nils Napp, Olga Wodo, and Jaroslaw Zola. Entropy-isomap: Manifold learning for high-dimensional dynamic processes. In *Proceedings of IEEE International Conference on Big Data*. IEEE, August 2018.
- Leland McInnes, John Healy, and James Melville. Umap: Uniform manifold approximation and projection for dimension reduction. *Journal of Open Source Software*, 3(29), September 2018.
- Ho T. Kam. Random decision forests. In *Proceedings of the 3rd International Conference on Document Analysis and Recognition*, pages 278–282, Montreal, Quebec, 1995. IEEE.